



## A structural traffic flow model for urban arterial roads

H. Qi<sup>1</sup>, D. Wang<sup>2,\*</sup>, P. Chen<sup>3</sup>, Y. Bie<sup>4</sup>

Received: February 2013, Revised: August 2013, Accepted: January 2014

### Abstract

A structural model for urban arterial roads traffic flow is proposed. It describes the road traffic dynamics in a disaggregated way. The structural model's main components are as follows: (1) A link traffic model that tracks the traffic waves cyclically: Traffic waves within each cycle are captured by three characteristic points. These points are formed when different traffic waves meet. (2) A proportional line model that is used to split the overall outflow into different turning flows: The model is derived directly from the first-in-first-out (FIFO) principle. (3) A spillover component that deals with channelized section queue overflow. (4) A traffic flow performance index component that outputs macroscopic and microscopic-level indexes. These indexes include delays, stops, queue lengths, vehicle trajectories, and travel times. The first three can be used in traffic flow optimization and the last two are valuable in vehicle emissions evaluation. Simulation results show that, with increasing numerical resolution, the traditional CTM (cell transmission model) gradually converges to our model.

**Keywords:** Arterial road, Traffic signal, Spillover, Performance indexes.

### 1. Introduction

Traffic flow modeling is an essential task in urban traffic management and planning. On the one hand, it provides an evaluation tool for traffic management plans; on the other hand, it serves as a forecasting input for traffic flow operations [1].

The arterial road is the key component of any road network. Traditionally, the arterial road is modeled by a link connecting two nodes [2]. There are four classes of such link models: (a) speed-density function models, wherein the movement of traffic is determined by the speed-density relationship; (b) bottleneck/queuing models [3], in which traffic congestion takes the form of queuing behind bottlenecks; (c) hydrodynamic models [4-6], in which traffic flow is governed by a hydrodynamic equation, and (4) whole-link function models [7] whose outflows are determined by link-scale measurements such as the number of vehicles in a link.

However, in urban areas, traffic flow behavior in arterial roads is more complex than a simple one-lane link. The complexity is threefold: (1) Firstly, the geometry of arterial roads is usually heterogeneous, both laterally and longitudinally. Traffic flow operates separately in channelized sections and is mixed in upstream sections. The number of lanes in the two sections may differ. (2) A signal control usually exists at the end of the arterial road. During peak hours, spillover events can result in unexpected traffic dynamics. (3) Different turning flows are likely to behave in different ways.

Arterial roads have been modeled using many methods. Wu and Liu [8] proposed a shockwave profile model. The wave was tracked during each numerical interval. The errors were found to be significant when the interval was large and the flow divergence was realized through a predefined ratio. Li [9] utilized the cell transmission model (CTM) [10] to establish equations for arterial road traffic dynamics. Their model can consider a spillover blockage but the turning percentage is exogenous, rather than being determined by the flow propagation. Liu and Chang [11] divided the arterial road into six subsets, including demand entries, upstream arrivals, joining the end of the queue, merging into lane groups, the departing process, and flow conservation. Each subset was described by a set of recursive equations.

\* Corresponding author: wangdianhai@sohu.com

1 Postdoctoral Research Fellow College of Civil Engineering, Zhejiang University, No. 388, Yuhangtang Road, Hangzhou, 310058, China

2 Professor, Dr.-Eng, College of Civil Engineering, Zhejiang University, No. 388, Yuhangtang Road, Hangzhou, 310058, China

3 Postdoctoral Research Fellow, Department of Civil Engineering, Nagoya University, Furo-cho, Chikusa-ku, Nagoya 464-8603, Japan

4 Lecturer, School of Transportation Science and Engineering, Harbin Institute of Technology, Harbin 150091, China

**Table 1** Summary of link traffic flow models

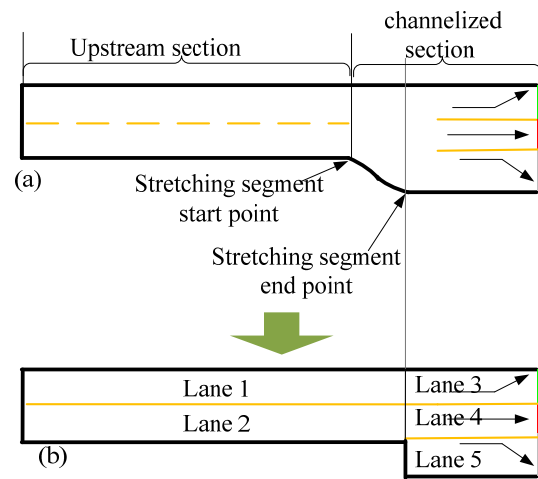
Model type	Feature	Link homogeneous?	Typical literature	
	Speed-density function	Single equation	yes	[13]
Link model	Bottleneck/ queuing model	Freely moving + queuing	no	[3]
	Hydrodynamic model	Analog to fluid	no	[4]~[6]
	Whole-link function model	Simplicity	yes	[7]
Others	CTM and its extension	Simulation for each cell in each interval	no	[9][10]
	CTM-like	Temporally based on intervals	no	[8][11]

Nonetheless, a highly efficient arterial loading road model is still lacking. This situation may partly be due to the analytical requirements of the model in a network framework. The outputs required from such models are varied as well. On the one hand, common traffic flow performances such as delays, queue lengths, and stops are required as the basis for operational evaluation and optimization [11]. On the other hand, microscopic-level variables such as travel time and trajectories are also of concern as they can be used for LOS (level of service) evaluations and emissions reduction [12]. With the current models it is difficult to satisfy these requirements simultaneously. We propose a structural model to address these problems. The model is based on traffic wave theory and decomposes the arterial road into a series of interconnected lanes. The model is temporally based on RGP (red-green-pair). The traffic state can be deduced iteratively rather than having to be tracked in each fixed numerical interval. The derivation of traffic dynamics is realized through three characteristic points and two characteristic moments of arrival. The three points depict the profile of the back of the queue, while the two moments of arrival limit the traffic demand within the cycle. Common traffic performance indexes such as delay, stops and queue length are also outputs of the model. This is particularly useful for network traffic evaluation and optimization. The turning ratio is modeled explicitly through the cumulative number of vehicles, rather than assumed to be a predefined value as it is in much research.

This paper is structured as follows: First of all, the decomposition method for the arterial road and the model structure are provided. Then, the lane traffic model is presented. Sections 3 to 7 present the respective components of the model. Next, a numerical study is carried out to demonstrate the capability of the model. Conclusions and future research directions are given in section 9.

## 2. Model Structure and Decomposition Method

The road is decomposed into a series of interconnected lanes as shown in Fig. 1. The road is divided into two sections: an upstream section and a channelized section. Each section is comprised of some lanes.

**Fig. 1** Decomposition of arterial road

Each lane performs as the input source or output destination of other lanes. The model structure contains five main parts:

a) The core component of the model is RGP-based traffic dynamics derivation. For signal-controlled lanes, RGP-based traffic dynamics tracking is realized through three characteristic points.

b) When channelized section spillover takes place, the exits of the upstream lanes (such as lane 1 in Fig. 1(b)) are blocked. A virtual signal is set at the exit, and an RGP model designed for signalized lanes is applicable. A model dealing with the spillover event is established as well.

c) The outflow determination component aims at deriving the outflow based on an RGP-based traffic dynamics model.

d) In many arterial models, the turning ratio of the channelized section entrance is assumed to be exogenously given. However, this assumption is questionable. A proportional line model based on a cumulative curve, derived from FIFO (first-in-first-out) is created to split the outflow of a lane.

e) More and more outputs are being expected from traffic flow models these days. The model structure includes a traffic performance model to meet this

requirement. This component produces macroscopic-level indexes such as delay, stops, and queue length, and microscopic-level variables such as vehicle trajectories and travel time.

The overall structure of the model is shown in Fig. 2. The structural model works as follows: the upstream section takes flow from the upstream intersection as

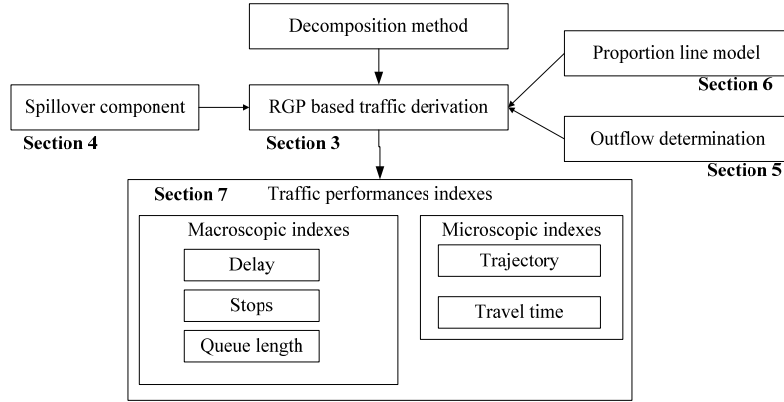


Fig. 2 Structural model for urban arterial road

### 3. RGP-Based Traffic Derivation

The method divides the time horizon into a series of consecutive RGPs according to the signal settings. Traffic dynamics for each RGP are captured through the traffic waves, and the waves themselves are confined by three characteristic points.

The fundamental diagram for the traffic flow is assumed to be the shape shown in Fig. 3. It is characterized by free-flow speed  $v_f$ , backward wave speed  $w$  and jam density  $k_{jam}$ .

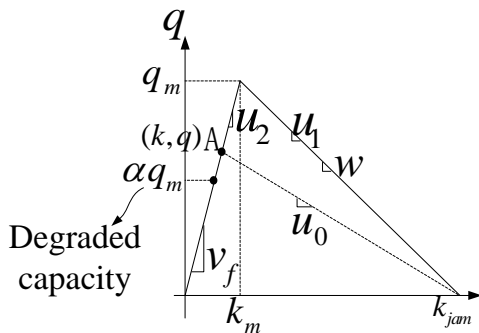


Fig. 3 Fundamental diagram

A typical RGP consists of a red time  $r$  and an effective green time  $g$ . Each RGP is called a cycle, which is slightly different from the traditional cycle concept. Fig. 4 presents the traffic wave profile of two typical cycles. In cycle  $i$ , after the beginning of the red time, a stopping wave  $u_0$  forms and propagates upstream. The velocity of the wave is determined by the arrivals. When the signal turns to green, a starting wave  $u_1$  forms and propagates upstream as well. The velocity of the

inputs, and outputs flow to the channelized section lanes; the channelized section lanes then accept these flows and release them at the stop line. The traffic flow dynamics of all these lanes are modeled by the RGP method. The output flow is then described by the outflow determination component. The model inputs are the directional flow and signal parameters, along with the road geometry.

starting wave is  $w$ . When the two waves meet, a new wave  $u_2$  comes into being. Its velocity is  $v_f$ . If the green time ends before the time at which wave  $u_2$  propagates across the stop line, a residual queue will exist for the next cycle and the current cycle is oversaturated.

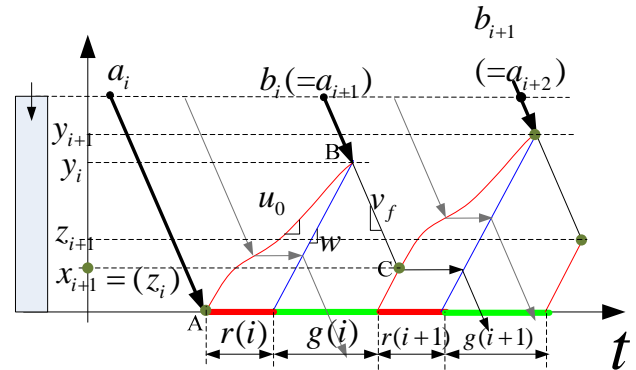


Fig. 4 traffic wave of two typical cycles

Within each cycle, we define three back of queue positions as characteristic points. For instance, in cycle  $i$ , the wave trajectory between points  $A$  and  $B$  represents a stopping wave, and that between  $B$  and  $C$  denotes the wave formed by the meeting of  $u_0$  and  $u_1$ . The spatial coordinates of  $A$ ,  $B$  and  $C$  are  $x_i$ ,  $y_i$  and  $z_i$  respectively and the temporal coordinates are  $t_x$ ,  $t_y$  and  $t_z$ . The three positions reflect the overall queue evolution in cycle  $i$ . Hence, they are called characteristic points. For cycle  $i+1$ , characteristic point  $x_{i+1}$  equals  $z_i$ . In this way, the traffic flow dynamics can be derived iteratively.



According to the traffic wave dynamics shown in Fig. 6,  $t_{z_i}$  can be formulated as

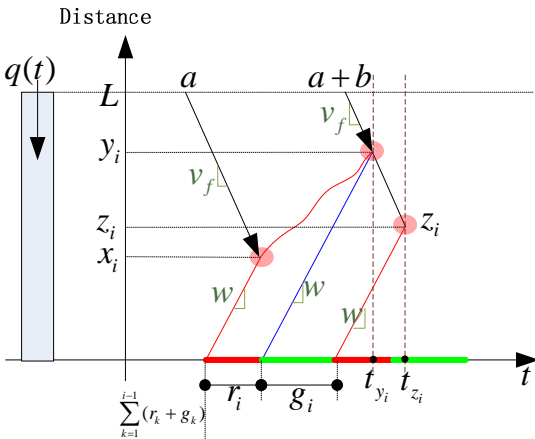


Fig. 6 traffic flow evolution from y to z

$$t_{z_i} = \sum_{k=1}^i (r_k + g_k) + \frac{z_i}{w} \quad (9)$$

$t_{z_i}$  can be derived from  $y_i$  as well:

$$t_{z_i} = t_{y_i} + \frac{y_i - z_i}{v_f} \quad (10)$$

The combination of Eq.(9) and Eq.(10) leads to the following formula:

$$z_i = \frac{wv_f \left( t_{y_i} + \frac{y_i}{v_f} - \sum_{k=1}^i (r_k + g_k) \right)}{w + v_f} \quad (11)$$

Thus,  $t_{z_i}$  is known from Eq.(10).

Because  $x_{i+1} = z_i$ , the traffic state can be computed iteratively, cycle by cycle.

### 3.3. Back of queue trajectory

Suppose we want to compute the real-time back of queue coordinate  $l_{AS}(t)$ . The moment  $t$  belongs to cycle  $i$ , i.e.

$$\sum_{k=1}^{i-1} (r_k + g_k) \leq t \leq \sum_{k=1}^i (r_k + g_k) \quad (12)$$

There is a time lag in the back of queue formation for the  $i$ -th cycle. Assume that the back of the queue at time  $t$  belongs to cycle  $j$  and it is recorded as  $j^*(i)$ . The characteristic points are  $x_{j^*(i)}$ ,  $z_{j^*(i)}$  and  $y_{j^*(i)}$  respectively. According to the relationship between  $t$  and  $t_{y_{j^*(i)}}$ , there are two cases, as shown in Fig. 7: case A and case B.

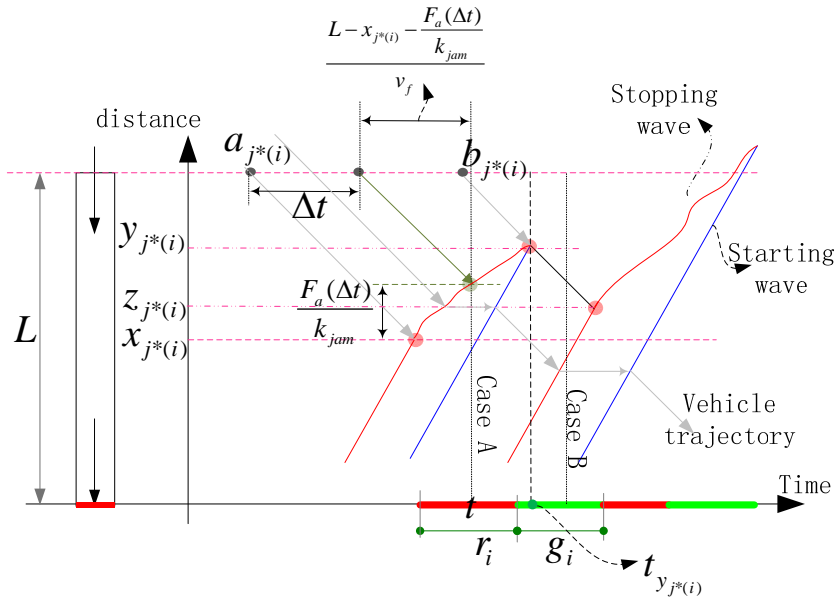


Fig. 7 queue back trajectory derivation

In case A, the vehicle enters the link and travels with speed  $v_f$  at time  $a_{j^*(i)} + \Delta t$  ( $\Delta t$  belong to the interval

$[0, b_{j^*(i)} - a_{j^*(i)}]$ ). The cumulative number of vehicles during  $[a_{j^*(i)}, a_{j^*(i)} + \Delta t]$  is



$$length_{y_k^N} = (t_{y_k} - t_{x_k} - r_k) \frac{y_k - L}{y_k - x_k} \quad (22)$$

Hence,

$$t_{y_k^u} = t_{y_k} - length_{y_k^N} = t_{y_k} - (t_{y_k} - t_{x_k} - r_k) \frac{y_k - L}{y_k - x_k} \quad (23)$$

Since  $l_{AS}(t_{y_k^u}) = L$ , we can simply express  $t_{y_k^u}$  as

$$t_{y_k^u} = l_{AS}^{-1}(L) \quad (24)$$

where  $l_{AS}^{-1}(\square)$  denotes the inverse function of  $l_{AS}(\square)$ .

Thus, the spillover interval is  $[l_{AS}^{-1}(L), t_{y_k} - (t_{y_k} - t_{x_k} - r_k) \frac{y_k - L}{y_k - x_k}]$ . Within the interval,

vehicles cannot enter the link and the upstream lane/link can be seen as a signal-controlled lane/link. All of the above models can be applied. It should be noted that there is a capacity drop which is caused by the interaction among flows in the upstream section. To address this problem, we introduce a coefficient  $\alpha$  ( $0 < \alpha \leq 1$ ) to capture the drop. The saturation flow in the upstream section when the downstream queue has been cleared is

$$\alpha q_m. \text{ The corresponding starting wave is } \frac{\alpha q_m}{k_{jam} - \alpha k_m}.$$

Other parameters are the same.

## 5. Outflow Determination

The outflow of a link depends on the signal display and the traffic states. If  $z_i = 0$ , it means that there is no residual queue. Therefore, during the green time in this cycle, after  $t_{z_i}$ , outflow  $q_O(t)$  becomes  $q_I(t - \frac{L}{v_f})$ .

Otherwise, during the effective green time, the outflow always equals the maximum flow rate.

It is easy to see that the computational complexity of our model is  $O(n)$ , where  $n$  is the number of RGP cycles. The computational complexity of other models that are based on a numerical interval is  $O(\frac{T}{\tau})$ , where  $\tau$  is the numerical interval and  $T$  is the study's time horizon.

## 6. Proportion Line Model

In much research, the diverging flow, or turning ratio at the entrance of the channelized section, is assumed to be given a priori [8]. However, this is not true when the demand is variable. Changes in the demand composition will inevitably result in a dynamic turning ratio. In this section, we propose a PLM (proportion line model) to address this issue. The PLM is derived directly from the

FIFO rule and is based on the cumulative number of vehicles, rather than the real-time flow rate.

### 6.1. Basic principle

**PROPOSITION:** Suppose a road is ruled by FIFO. Then, wherever we count the cumulative flow from a pre-given value, the ratio of the increments for different routes will always be the same.

**Proof:** Suppose we examine cumulative flow on two routes, say,  $i$  and  $j$ , at two positions  $x_1$  and  $x_2$ . When the cumulative flow on route  $j$  at  $x_1$  is  $n_j$ , suppose the cumulative flow on route  $i$  at  $x_1$  is  $n_i$ . When the  $n_j$ -th vehicle on route  $j$  arrives at  $x_2$ , according to the FIFO principle, all vehicles arriving earlier than the  $n_j$ -th vehicle at  $x_1$  will already have passed  $x_2$ , and all vehicles arriving later than the  $n_j$ -th vehicle at  $x_1$  will not yet have reached  $x_2$ , meaning that the cumulative flow for route  $i$  will be  $n_i$  when the cumulative flow for route  $j$  is  $n_j$ . In other words, if we express  $\Delta A_i$  as  $g(\Delta A_j)$ , where  $\Delta A$  is the cumulative increment in the number of vehicles, then the relationship  $g(\Delta A_j)$  is independent of location. This relationship will be called the proportion line hereafter. Below, a discrete form of cumulative determination model is given.

### 6.2. Discrete form

For the sake of simplicity, consider flow  $q_k$  as shown in Fig. 9, which consists of flow  $q_i$  and  $q_j$ , i.e.  $q_k(t) = q_i(t) + q_j(t)$ . When the spatial factor is considered, it leads to  $q_k^x(t) = q_i^x(t) + q_j^x(t)$ . The relationship also holds true for cumulative vehicle numbers, i.e.  $A_k^x(t) = A_i^x(t) + A_j^x(t)$ . Suppose the downstream capacity for route  $i$  is  $\bar{q}_i(t)$  and similarly we have  $\bar{q}_j(t)$ . They are assumed to be fixed during interval  $\tau$  (there is no further constraint upon  $\tau$ ; in other words,  $\tau$  need not be a constant). The cumulative increment limits for routes  $i$  and  $j$  are  $\Delta \bar{A}_i$  ( $= \bar{q}_i(t) \times \tau$ ) and  $\Delta \bar{A}_j$  ( $= \bar{q}_j(t) \times \tau$ ) respectively. If the overall outflow is also confined by a capacity  $\bar{q}(t)$ , the overall cumulative increment limit is  $\Delta A_m$  ( $= \bar{q}(t) \times \tau$ ).

The three constraints are displayed in Fig. 10. The feasible solutions for  $\Delta A_i$  and  $\Delta A_j$  must drop into the shadowed area surrounded by the constraint lines.

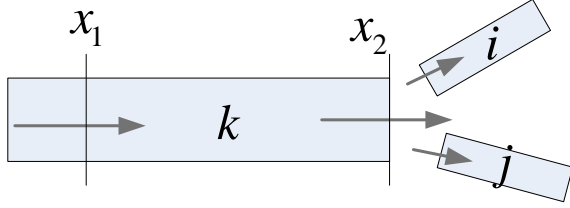


Fig. 9 turning ratio determination

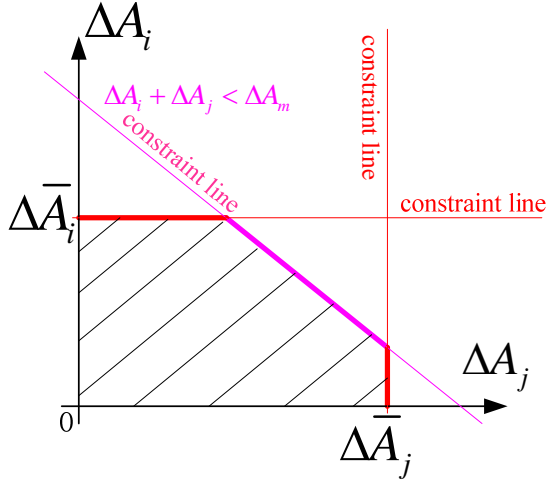


Fig. 10 Capacity constraint lines

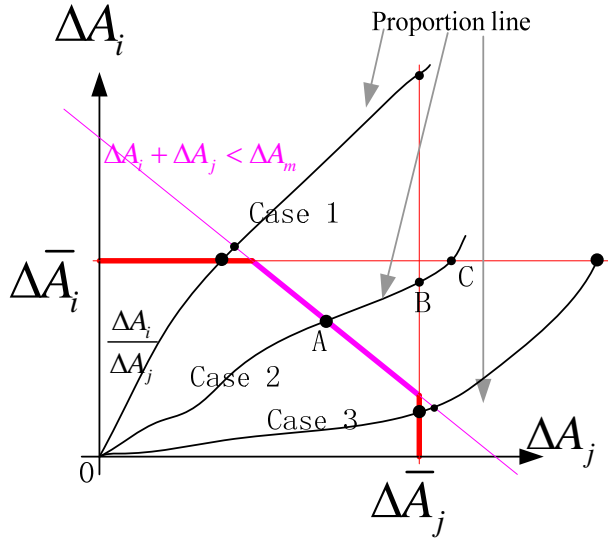


Fig. 11 Solving of outflow

According to the proposition, the cumulative increment is depicted by the proportion line. Fig. 11 presents three cases for the flow comprised of two route flows. Taking case 2 as an example, the proportion line intersects with the three constraint lines at three points: A, B and C. Since the outflow will maximize itself and must be in the shadowed area, the ultimate result must be A. It is found that, whichever case we look at, the result is always the point where the proportion line intersects with the

boundary denoted by the bold line. This can be expressed uniformly as

$$A_k^{x_2}(t+\tau) = \min\{A_k^{x_2}(t) + \Delta A_m, A_k^{x_2}((A_i^{x_1})^{-1}(A_i^{x_2}(t) + \Delta \bar{A}_i)), A_k^{x_2}((A_j^{x_1})^{-1}(A_j^{x_2}(t) + \Delta \bar{A}_j))\} \quad (25)$$

where  $(A_i^{x_1})^{-1}(\bullet)$  is the inverse function of  $A_i^{x_1}(t)$ .  $A_i^{x_2}(t) + \Delta \bar{A}_i$  denotes the expected cumulative number of vehicles on route  $i$ . Hence, the term  $(A_i^{x_1})^{-1}(A_i^{x_2}(t) + \Delta \bar{A}_i)$  denotes the arriving moment at  $x_1$  for the last vehicle of the expected departing flow on route  $i$ . The first term in the curly brackets denotes point A and, by parity of reasoning, C, B.

Eq.(25) indicates that the result is the minimum of the three intersection points between the proportion line and the constraint lines.

The cumulative number of vehicles for the different routes are

$$A_i^{x_2}(t+\tau) = A_i^{x_1}((A_k^{x_1})^{-1}(A_k^{x_2}(t+\tau))) \quad (26)$$

$$A_j^{x_2}(t+\tau) = A_j^{x_1}((A_k^{x_1})^{-1}(A_k^{x_2}(t+\tau))) \quad (27)$$

The flow rates are

$$q_i^{x_2}(t+\tau) = \frac{dA_i^{x_2}(t+\tau)}{dt} \quad (28)$$

$$q_j^{x_2}(t+\tau) = \frac{dA_j^{x_2}(t+\tau)}{dt} \quad (29)$$

The method can easily be extended to a flow that consists of multiple routes, using the generalized formula:

$$A_k^{x_2}(t+\tau) = \min\{A_k^{x_2}(t) + \Delta A_m, A_k^{x_2}((A_i^{x_1})^{-1}(A_i^{x_2}(t) + \Delta \bar{A}_i))\}, \forall i \quad (30)$$

In the computation, linear interpolation may be necessary.

## 7. Traffic performance indexes

### 7.1. Delay, stops and queue length

Traditionally, three indexes have been the subject of traffic optimization and evaluation, namely delay, stops and queue length. During off-peak hours, the first two are the major objectives, while the final one dominates under rush-hour circumstances. Here, they are derived from the outputs of the models described above.

The traffic wave profile is shown in Fig. 12. The horizontal distance between curve ABC and line CE represents vehicle delay. Therefore, overall delay, which is the sum of the single vehicle delays, is the area of polygon AEDCBA, multiplied by the jam density,  $k_{jam}$ :

$$d_i = x_i r_i k_{jam} + k_{jam} \left[ \int_{t_{x_i}}^{t_{y_i}} (l_{AS}(t) - x_i) dt - \frac{(t_{y_i} - t_{x_i} - r_i)(y_i - x_i)}{2} \right] \quad (31)$$

Maximal queue length during cycle  $i$  is

$$l_i = y_i \quad (32)$$

Since each vehicle that joins the back of the queue will stop once it is within the cycle, and the overall number of stopped vehicles is  $y_i k_{jam}$ , the number of stops  $S_i$  during cycle  $i$  is

$$S_i = y_i k_{jam} \quad (33)$$

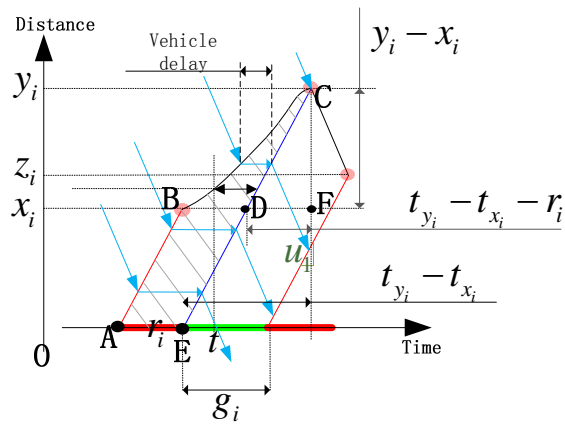


Fig. 12 derivation of traffic index

### 7.2. Vehicle trajectory and travel time

The velocity of the vehicle is either zero or the free-flow speed. The traffic wave is formed by the change in the vehicle's velocity. Thus the vehicle's trajectory can easily be judged when the traffic wave is given. The reconstruction of the vehicle's trajectory is omitted here. Fig. 13 presents the trajectories of three typical vehicles.

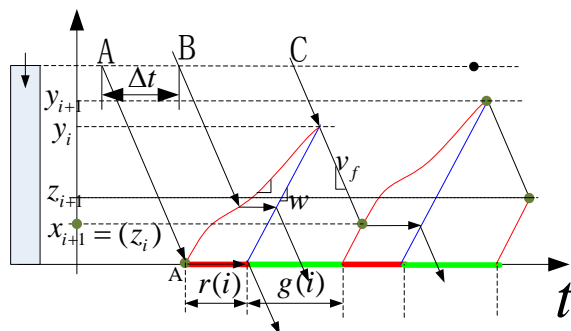


Fig. 13 Trajectories of three typical vehicles

Travel time can be obtained in two ways. If the vehicle's trajectory is given, the travel time is the time difference between the moment it enters and the moment it exits. The second way is the cumulative vehicle method. The cumulative curve for the inflow is given as we know the conditions, and that for the outflow is derived from the outflow determination component. Thus, the horizontal difference between the two curves is the travel time.

## 8. Numerical Simulation

In this section, we present a numerical example to demonstrate the capabilities of our model. The simulation is carried out on an arterial road as shown in Fig. 14. It consists of two sections: an upstream section and a channelized section. There are two lanes in the upstream section and three in the channelized section. The lengths of each section are labeled in the figure.

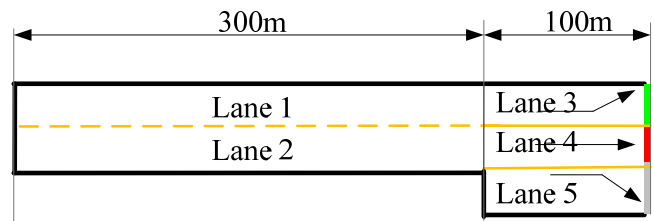


Fig. 14 Simulation test bed

The fundamental diagram parameters are set as follows:  $v_f=40km/h$ ;  $w=20km/h$ ;  $k_j=130veh/km$ .

Capacity degradation coefficient  $\alpha$  is set to 0.5, i.e. the degraded capacity is about 866.7veh/h. The cycle length is 90s. The green times for the left-turning flow and the through flow are both 30s. The through flow phase follows the left-turn phase. Fig. 15 shows the simulation demand. In order to examine the model's capability for reproducing arterial road dynamics under different demand structures, the peak hours for different turning directions are separated. For each entering lane, the overall demand is shown on the right of Fig. 15.

Fig. 16 shows the wave profiles for the left-turning flow and the through flow. At first, there is no initial vehicle on the road, and the queue length is thus very short. With the increase in demand, the left-turning flow queue firstly increases and reaches the peak level. Spillover of the left-turning queue within the channelized section hence occurs. The spillover event lasts for four time steps. The intervals are listed in Table 2.

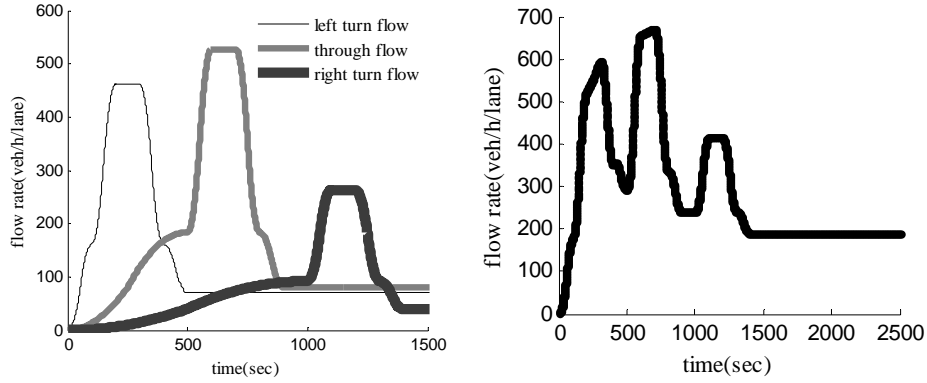


Fig. 15 Simulation demand, left: for each turning direction; right: overall

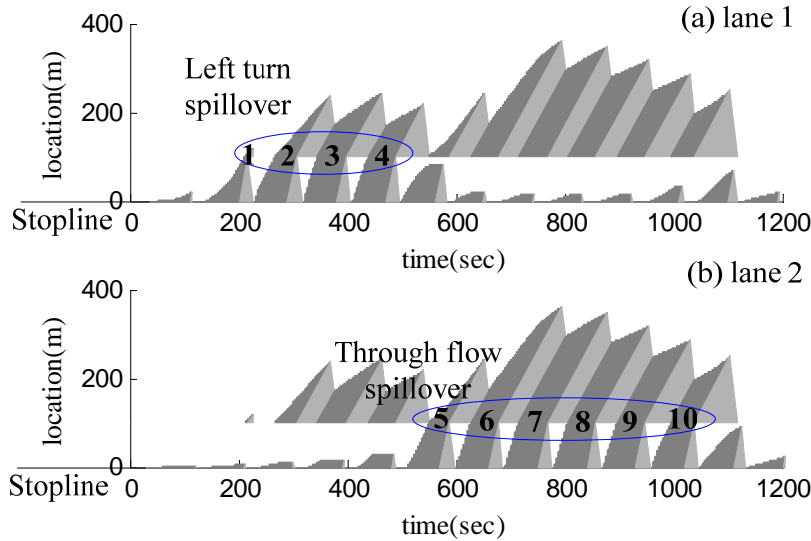


Fig. 16 traffic wave profiles

Table 2 Spillover interval of left-turning flow

Spillover cycle	1	2	3	4
Starting time (s)	211.1	267.0	344.3	438.6
Ending time (s)	218.0	308.0	398.0	488.0

The peak hour of through flow follows, which results in through queue spillover. Since the demand for the through flow is higher than that for the left-turn, the spillover event lasts for six time steps as listed in Table 3. During these time intervals, vehicles turning left cannot enter the turning lane either.

Table 3 Spillover interval of through flow

Spillover cycle	5	6	7	8	9	10
Starting time (s)	549.9	626.3	714.7	805.1	895.7	995.7
Ending time (s)	588.0	678.0	768.0	858.0	948.0	1038.0

Fig. 17 and Fig. 18 present the wave profile as well as the trajectories of each vehicle, for both left-turning flow and through flow. During the spillover interval, vehicles cannot enter the downstream section even if there is

enough space. From the waves and trajectories, five traffic states can be recognized. State A represents the arrival traffic flow and B denotes the jam state where the vehicle velocity is zero. E and C denote the releasing flow for the upstream section and channelized section respectively. Due to the capacity drop, the flow of traffic state B is smaller than that of E. The difference is determined by the drop intensity. In traffic state D, there are no vehicles. However, upstream demand is sufficient. These traffic flows cannot enter the channelized section's lanes because the entrance is blocked by the spillover queue (in this case, it is blocked by the through vehicle queue). Hence, the density and flow of the traffic state are both zero.

Fig. 19 presents the outflow of the upstream lane. If there is no spillover, the outflow of the upstream lane should be a temporal shift of the arterial road's inflow, i.e. see Fig. 15. Because of the blockage caused by the spillover, the outflow in some moments decreases to zero. When the downstream queue is cleared, the releasing flow is 866.67, which is the maximal flow rate multiplied by the degradation coefficient. Fig. 20 displays the inflow of the turning lane in the channelized section. The inflow is regulated by the virtual signal at the entrance to the channelized section.

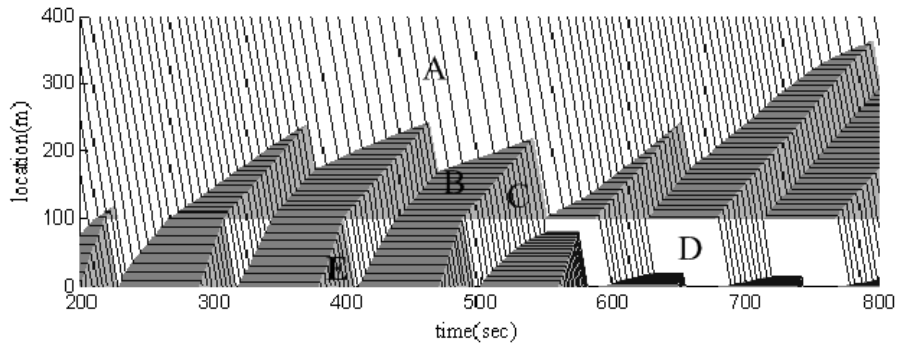


Fig. 17 Wave and trajectory of each vehicle for left-turn flow

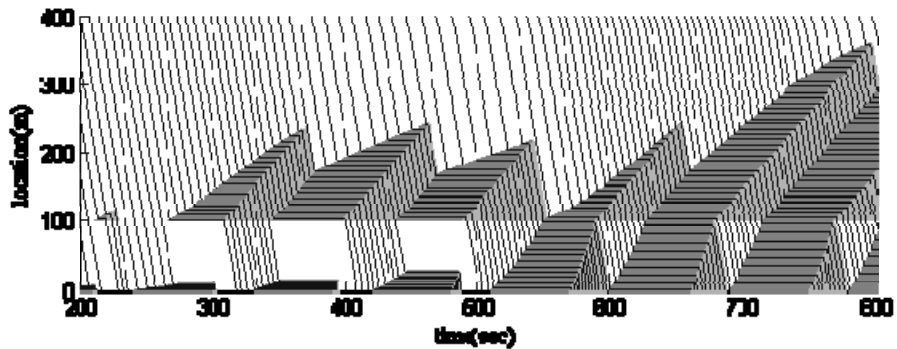


Fig. 18 Wave and trajectory of each vehicle for through flow

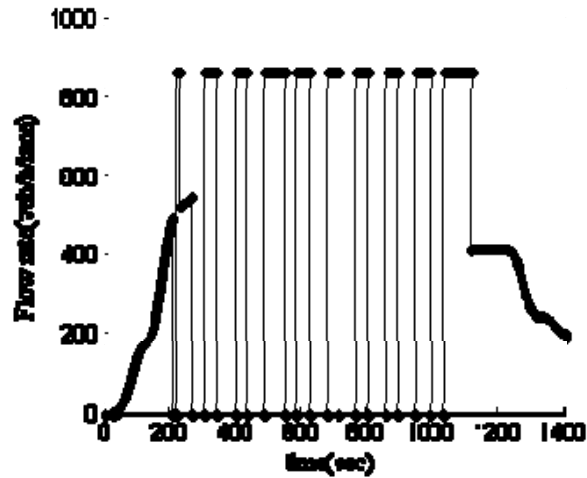


Fig. 19 Outflow of upstream section lane

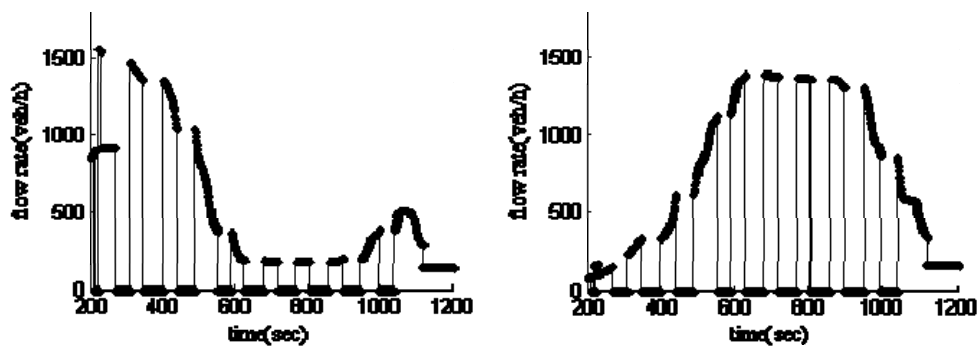


Fig. 20 Inflow rate for channelized section

The CTM (cell transmission model) [10] is a relatively efficient macroscopic traffic flow model. It is a discrete form of the LWR (Lighthill-Richards-Whitham) model. The CTM divides the road into a series of "cells". During each simulation interval, every cell receives traffic flow from the upstream cell and outputs traffic flow to the downstream cell. Then, the traffic dynamics can be tracked iteratively. Generally, this model will generate more accurate results when the cell length is short. In this example, for comparison, we chose two different cell lengths: 10m, corresponding to a time interval of 0.9s, and 20m, corresponding to a time interval of 1.8s. The other parameters are the same as above. Because there is no turning ratio determination model for the CTM, in the simulation this is determined by our model based on the cumulative number of vehicles.

Fig. 21 and Fig. 22 present the density profiles of the

left-turning lane and the through lane under the two different cell lengths. The cell length in Fig. 21 is 10m and that in Fig. 22 is 20m. From the profiles, it can be seen that (1) our model and the CTM can both simulate the arterial road traffic evolution over time, and since our model does not need to divide the road into cells and track the traffic flow in each numerical interval, the computational efficiency is surely higher. (2) A smaller cell length can track traffic flow dynamics more precisely but at the cost of computational efficiency. Fig. 23 displays the output flow at the stop line for both models. Our model produces similar results to the CTM model, and has the capability to derive vehicle trajectories and performance indexes. (3) The proposed model can explicitly calculate the back of the queue while, in the CTM, it must be identified by a pre-defined density upper bound.

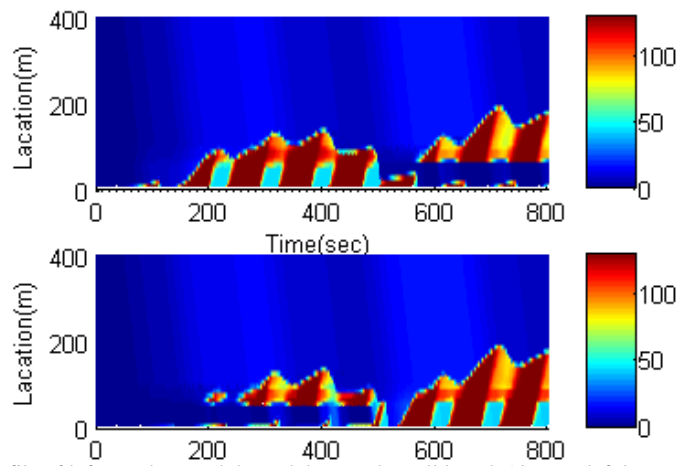


Fig. 21 Density profile of left-turn lane and through lane under cell length 10m up: left lane; down: through lane

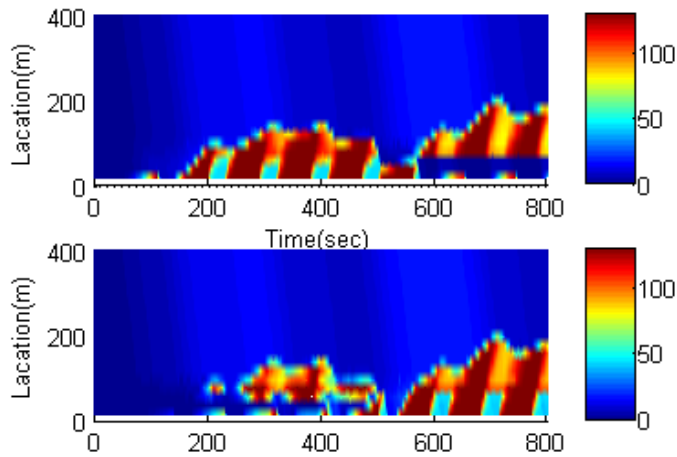
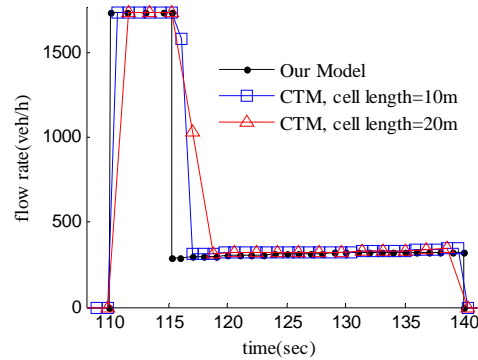


Fig. 22 Density profile of left-turn lane and through lane under cell length 20m up: left lane; down: through lane



**Fig. 23** Departure flow of left-turn lane comparison

The proposed model is of the macroscopic type. Computational efficiency is assured based on the spatial and temporal scale. At the same time, various traffic flow indexes can be derived. Besides this, vehicle trajectories are also useful for emissions modeling. Thus, our model is suitable for traffic management, such as the optimization of signal parameters, channelized section design, capacity analysis considering spillovers, etc. However, since spillovers involve not only macroscopic traffic features but also microscopic driver behavior, the spillover description in the model can only approximate the real world. This can be solved by adjusting the capacity drop coefficient, calibrating it to field data.

## 9. Conclusion

A novel, highly efficient structural model for arterial roads, based on shockwave theory, is proposed. Unlike existing models, the proposed model spatially divides the road into a series of lanes, and temporally tracks the traffic dynamics based on each RGP. Since the spillover is viewed as a virtual signal, all lanes are modeled uniformly. Common traffic performance indexes can be derived directly. This is especially useful for optimization and evaluation.

Some issues that we are investigating further are the following: (1) The capacity degradation is influenced by macroscopic variables such as flow composition, and also relates to the drivers' microscopic behavior. Calibration should be considered. (2) Shared lanes exist on some arterial roads. The utilization of these lanes may influence the road traffic dynamics. The inflow composition of the channelized section needs to be incorporated. (3) Spillover events actually develop gradually, rather than immediately blocking the entrance to the channelized section. This can be modeled by including a relaxation coefficient.

## References

[1] Hofleitner A, Herring R, Bayen A. Arterial travel time forecast with streaming data: A hybrid approach of flow modeling and machine learning, *Transportation Research Part B: Methodological*, 2012, No. 9, Vol. 46, pp. 1097-1122.

[2] Li C, et al. A global optimization method for continuous network design problems, *Transportation Research Part B: Methodological*, 2012, No. 9, Vol. 46, pp. 1144-1158.

[3] Ban X, et al. Continuous-time point-queue models in dynamic network loading, *Transportation Research Part B: Methodological*, 2012, No. 3, Vol. 46, pp. 360-380.

[4] Lighthill MJ, Whitham GB. On kinematic waves II. A theory of traffic flow on long crowded roads, *Proceedings of the Royal Society A*, 1955, Vol. 229, pp. 317-345.

[5] Whitham G.B. *Linear and Nonlinear Waves*, New York, Wiley, 1974.

[6] Chen Jz, Zk Shi, YM Hu. A relaxation scheme for a multi-class lighthill-whitham-richards traffic flow model, *Journal of Zhejiang University Science A*, 2009, No. 22, Vol. 10, pp. 1835-1844.

[7] Carey M, Ge YE, McCartney M. A whole-link travel-time model with desirable properties, *Transportation Science*, 2003, No. 1, Vol. 37, pp. 83-96.

[8] Wu X, HX Liu. A shockwave profile model for traffic flow on congested urban arterials, *Transportation Research Part B: Methodological*, 2011, No. 10, Vol. 45, pp. 1768-1786.

[9] Li ZC. Modeling arterial signal optimization with enhanced cell transmission formulations, *Journal of Transportation Engineering-Asce*, 2011, No. 7, Vol. 137, pp. 445-454.

[10] Daganzo CF. The cell transmission model: A dynamic representation of highway traffic consistent with the hydrodynamic theory, *Transportation Research Part B: Methodological*, 1994, No. 4, Vol. 28, pp. 269-287.

[11] Liu Y, GL Chang. An arterial signal optimization model for intersections experiencing queue spillback and lane blockage, *Transportation Research Part C: Emerging Technologies*, 2010, No. 1, Vol. 19, pp. 130-144.

[12] Stevanovic A, et al. Optimizing traffic control to reduce fuel consumption and vehicular emissions, *transportation research record, Journal of the Transportation Research Board*, 2009, Vol. 2128, pp.105-113.

[13] Edie LC. Discussion of traffic stream measurements and definitions, *Proceedings of the Second International Symposium on the Theory of Traffic Flow*. J. Almond (Editor), Paris, OECD, 1965, pp. 139-154.